Proc. Natl. Acad. Sci. USA
Vol. 91, pp. 1428–1432, February 1994
Biophysics

Structure of S-lectin, a developmentally regulated vertebrate β-galactoside-binding protein

DER-ING LIAO*, GEETA KAPADIA*, HAFIZ AHMED†, GERARDO R. VASTA†, AND OSNAT HERZBERG*‡

*Center for Advanced Research in Biotechnology, University of Maryland Biotechnology Institute, 9600 Gudelsky Drive, Rockville, MD 20850; and †Center of Marine Biotechnology, University of Maryland Biotechnology Institute, 600 East Lombard Street, Baltimore, MD 21202

Communicated by Wayne A. Hendrickson, October 18, 1993

ABSTRACT **The crystal structure of a 14-kDa bovine spleen S-lectin complexed with the disaccharide *N*-acetyllactosamine at 1.9-Å resolution reveals a surprising structural relationship to legume lectins, despite the lack of sequence homology. Two monomers associate to form an extended β-sandwich, each with the same jelly roll topology typical of legume lectins but with dramatically trimmed loops and with different dimer association. Each monomer binds one *N*-acetyllactosamine molecule in a topologically and spatially different site than that of legume lectins. The carbohydrate-binding site provides an unprecedented paradigm for carbohydrate binding, with a unique network of salt bridges. The specificity for β-galactose arises from intricate interactions that constrain the position of the O4 atom.**

Within the animal lectins two major groups have been defined, the S type (calcium-independent) and C type (calcium-dependent) (1). The S-lectins, found in all vertebrate species studied so far, are soluble, β-galactoside-specific binding proteins. There are at least three distinct classes of macromolecules in this family, the 14-kDa lectins, usually present in solution as noncovalently bound dimers and the larger members of 29- to 35-kDa and 67-kDa molecular mass (2). Each of the higher-molecular-mass proteins that have been sequenced contains a domain that has sequence homology to the 14-kDa proteins. The expression and cellular distribution of these cytosol-synthesized proteins are developmentally regulated (3). They require the presence of thiol reducing reagents both to retain *in vitro* carbohydrate-binding activity and to prevent covalent dimerization.

S-lectins have been implicated in diverse processes such as embryonic development, connective tissue regulation, organization of the nervous system, tumor development, and immune regulation (2). However, their function is not well understood. Because of their preferential binding to *N*-acetyllactosamine [Gal(β1 → 4)GlcNAc], it has been suggested that the function of S-lectin is mediated by binding to extracellular matrix proteins such as laminin and fibronectin, and to lysosomal-associated membrane proteins carrying the glycans containing multiple *N*-acetyllactosamine subunits (4–7). A high concentration of S-lectins has been demonstrated to reduce cell-substrate adhesion *in vitro* (8, 9). The growth inhibitory activity of mouse embryonic fibroblasts has been attributed to a 14-kDa S-lectin, unusually insensitive to oxidation (10). It has been proposed that the members of the S-lectin family are multifunctional molecules that may exhibit various biological roles in different tissues (2).

Biochemical, biophysical, and mutagenesis studies of S-lectins attempting to define the carbohydrate-recognition domain and to reveal the role of the conserved amino acid residues have been reported (11–14). The positions and conformations of hydroxyl groups on the preferred ligand of bovine spleen S-lectin were investigated by solid-phase-binding inhibition (H.A. and G.R.V., unpublished data) and exhibited the same characteristics as other 14-kDa S-lectins (11). Chemical-modification studies of the active protein have identified the nature of the amino acids involved in the carbohydrate-binding activity (H.A. and G.R.V., unpublished data), consistent with previous site-directed mutagenesis studies (14). Here, we report a high-resolution crystal structure of the 14-kDa S-lectin from bovine spleen complexed with *N*-acetyllactosamine.§

EXPERIMENTAL METHODS

Protein Purification and Crystallization. The protocol for the purification of the 14-kDa bovine spleen lectin will be described elsewhere (N. E. Fink, H.A., and G.R.V., unpublished results). Single crystals of the *N*-acetyllactosamine-bound lectin were obtained at room temperature by vapor diffusion in hanging drops. Protein drops were equilibrated against reservoir solutions containing 54–58% saturated ammonium sulfate, 100 mM Tris acetate (pH 6.6), and 0.5–2% (vol/vol) 2-methyl-2,4-pentanediol. The drops consisted of protein at 10 mg/ml, 1 mM *N*-acetyllactosamine, and 2 mM dithiothreitol, diluted with an equal volume of reservoir solution. Addition of *N*-acetyllactosamine is essential for the lattice formation. The space group of the crystals is $P2_12_12_1$. The unit cell dimensions are as follows: a = 59.3 Å, b = 62.9 Å, c = 70.1 Å. There are two lectin monomers in the asymmetric unit, and the solvent content of the crystal is ≈45% by volume. The crystals diffract to at least 1.85-Å resolution.

Structure Determination. The structure was determined at 2.7-Å resolution by the multiple isomorphous replacement method and refined at 1.9-Å resolution. X-ray-diffraction data were collected on a Siemens area detector mounted on a 3-circle goniostat, with monochromated CuKα x-rays supplied by a Rigaku Rotaflex RU200BH rotating anode generator. Native data were first collected at 2.1-Å resolution. Later, when a larger crystal became available, a new data set was obtained at 1.9-Å resolution. Heavy-atom derivative data were collected at 2.7-Å resolution. The data were processed by using the XENGEN package (15). The computer program packages PHASES¶ and PROTEIN (16) were used for heavy-atom parameter refinement and multiple isomorphous replacement phase calculation. A phase set with a mean figure of merit of 0.67 was derived from four heavy-atom derivatives. The final statistics of the crystallographic phase determination are summarized in Table 1. The 2.7-Å electron-density map calculated with these multiple isomorphous replacement

The publication costs of this article were defrayed in part by page charge payment. This article must therefore be hereby marked "*advertisement*" in accordance with 18 U.S.C. §1734 solely to indicate this fact.

Abbreviation: EcorL, *Erythrina corallodendron* lectin.

‡To whom reprint requests should be addressed.

§The atomic coordinates have been deposited in the Protein Data Bank, Chemistry Department, Brookhaven National Laboratory, Upton, NY 11973 (reference 1SLT).

¶Furey, W. & Swaminathan, S., 14th American Crystallographic Association Meeting, April 8–13, 1990, New Orleans, abstr. PA 33.

Table 1. Crystallographic statistics

Data set	Resolution, Å	Observations, no.	Unique reflections	R_{merge}*, %	Completeness	Sites, no.	R_{iso}*	R_{cen}*	$\langle f_h \rangle / \langle E_h \rangle$†
Native 1	2.1	53,805	14,741	9.2	0.92				
Native 2	1.9	84,959	20,694	6.4	0.98				
Hg01‡	2.7	23,225	14,844	4.5	0.82	8	0.39	0.63	1.64
Hg02‡	2.7	29,979	12,798	6.8	0.88	4	0.30	0.58	2.46
Ua02‡	2.7	26,892	12,686	4.9	0.87	4	0.16	0.62	1.02
Ua03‡	2.7	14,728	10,257	5.4	0.70	8	0.21	0.63	1.37

‡Crystal soaking conditions were as follows: Hg01, 1 mM methylmercuric chloride in mother liquor consisting of 62% saturated ammonium sulfate/2% 2-methyl-2,4-pentanediol/100 mM Tris acetate, pH 6.5 (28 hr); Hg02, same as for Hg01 but shorter soaking time (5 hr); Ua02, 3 mM uranyl acetate in the same mother liquor (27 hr); Ua03, 6 mM uranyl acetate in the same mother liquor (2 days).

*$R_{merge} = \Sigma_h |I_h - \langle I_h \rangle| / \Sigma_h I_h$; $R_{iso} = \Sigma_h ||F_{PH}obs| - |F_P obs|| / \Sigma_h |F_P obs|$; $R_{cen} = \Sigma_{h\ centric} ||F_{PH}obs| - |F_P obs + F_H cal|| / \Sigma_{h\ centric} ||F_{PH}obs| - |F_P obs||$, where I = intensity; h = Miller indices; obs = observed; cal = calculated; F_P, F_{PH}, and F_H = native protein (native 1), derivative protein, and heavy-atom structure factors, respectively.

†$\langle E_h \rangle$ = rms lack-of-closure error; $\langle f_h \rangle$ = rms heavy-atom scattering.

phases was of sufficient quality to trace the polypeptide chain. Map interpretation and model fitting were done by using the programs FRODO with the BONES feature (17, 18). The S-lectin dimer occupies the asymmetric unit. The initial map enabled modeling of 245 out of 268 residues constituting the physiological S-lectin dimer. The crystallographic R factor of this first model was 42.3% for data between 6.0 Å and 2.7 Å, for which $F \geq 2\sigma(F)$ ($R = \Sigma_h ||F_o| - |F_c|| / \Sigma_h |F_o|$, where $|F_o|$ and $|F_c|$ are the observed and calculated structure factor amplitudes, respectively).

Molecular dynamics refinement was done first, at 2.1-Å resolution, by using the slow-cooling protocol of X-PLOR at 3000 K (19); this was followed by restrained-parameter least-squares refinement using the program TNT (20). The two *N*-acetyllactosamine molecules were added after the first round of least-squares refinement. After a few cycles, a 1.9-Å data set was obtained, and the refinement proceeded with these data.

The bovine spleen lectin sequence has not yet been determined. However, the bovine fibroblast and heart lectin sequences are almost identical (21). Thus, it was assumed that spleen and heart lectin sequences are also similar. Indeed, the electron density is consistent with the sequence of bovine heart S-lectin. The difference-Fourier map of the mercurial derivative, HG01, indicated that all of the six putative cysteines bound mercury. Therefore, the thiol groups were presumably reduced. However, the crystal used to obtained the 1.9-Å data was 1 mo older than all other crystals, and the electron density of the model indicates that the side chains of the Cys-16, Cys-88, and Cys-130 are oxidized.

RESULTS AND DISCUSSION

Quality of the Structure. The refined model consists of 133 amino acid residues in one monomer and 132 amino acid residues in the other monomer, two *N*-acetyllactosamine molecules, and 154 water molecules. The conventional R factor of the model is 16.7% for the 18,460 reflections between 6.0 Å and 1.9 Å with $F \geq 2\sigma(F)$. The root-mean-square deviations (rms) from ideal bond lengths and angles are 0.018 Å and 3.9°, respectively. The electron-density map in the region of the carbohydrate-binding site is shown in Fig. 1.

Overall Structure of S-Lectin. The S-lectin dimer forms a 22-strand anti-parallel β-sandwich, with the N and C termini of each monomer at the dimer interface (Fig. 2). The two molecules are related to each other by a noncrystallographic 2-fold rotation perpendicular to the β-sheets. The structure reveals that there is one carbohydrate-binding site per monomer, in agreement with the results obtained from thermodynamic measurements. [Thermodynamic measurements indicate that there is one carbohydrate-binding site per monomer with an association constant of 10^5 M^{-1} for 4-methylumbel-

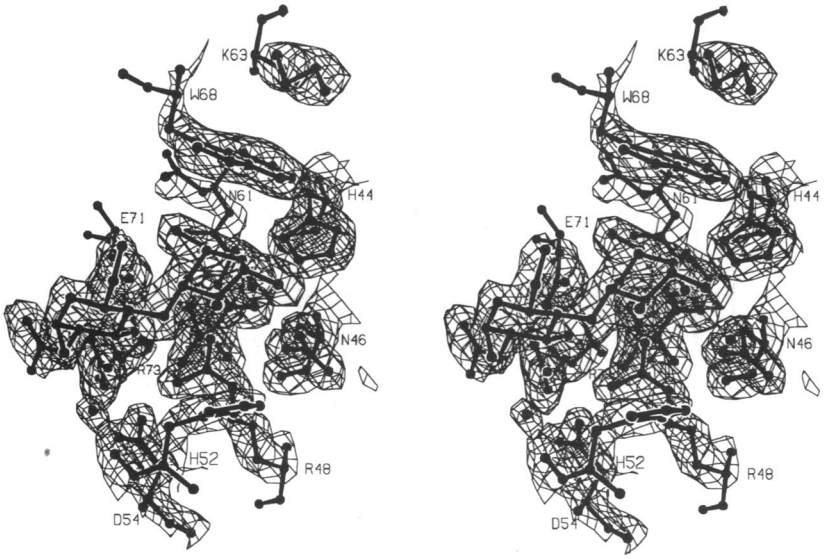

FIG. 1. Stereoscopic view of a region of the electron-density map in the vicinity of the carbohydrate-binding site. The refined 1.9-Å map with calculated phases and coefficient $2F_o - F_c$. The map is contoured at 1.1σ level.

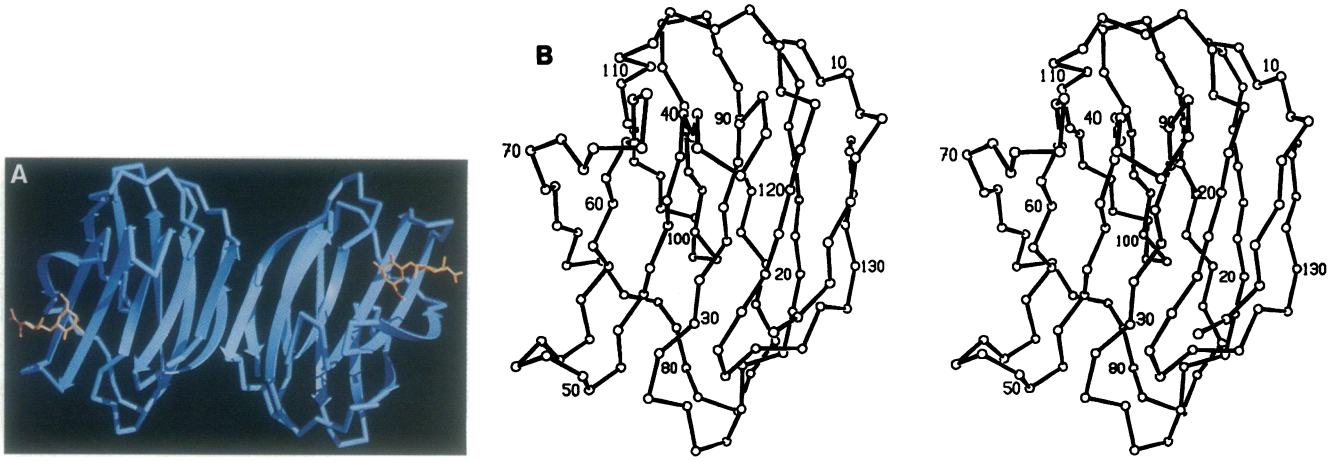

FIG. 2. Fold of S-lectin. (*A*) Highlighting secondary structure motifs of the dimer: β-strands are shown as ribbons, and the *N*-acetyllactosamine molecules are shown as yellow stick models. The model was generated by the computer program RASTER3D written by David Bacon (University of Alberta, Canada). (*B*) Stereoscopic representation showing the α-carbon positions of the monomer in the same orientation as the left-hand monomer in *A*. Every 10th amino acid is labeled. Secondary structure analysis using the DSSP program (22) shows the following residues to be in β-strands: 4–7, 16–23, 30–37, 40–51, 54–64, 67–74, 83–91, 95–99, 105–109, 119–124, and 126–132.

liferyl α-D-galactoside (H.A. and G.R.V., unpublished data)]. The two binding sites are located on the same side of the β-sandwich and on the far ends of the dimer 46 Å apart. The integrity of the dimer is maintained by the β-sheet interactions across the monomers and by the formation of a hydrophobic core common to both. There is no resemblance between the folds of the S-lectin and that of the carbohydrate-binding domain of the rat mannose-binding protein, a C-lectin that shows no significant sequence homology to the S-lectin (23). Thus, both primary and tertiary structures suggest that the two animal lectins are unrelated. Despite the lack of sequence homology, the crystal structure of the S-lectin reveals a fold with the same jelly roll topology as that of the legume lectins, but with the first and second parallel β-strands omitted (Fig. 3*A*). This jelly roll motif, shared by the two lectin families, contains a β-hairpin insertion unlike any other known jelly roll protein structures. The α-carbon atoms of the S-lectin were superposed on the three well-refined structures of legume lectins, Con A (24–26), *Erythrina corallodendron* lectin (EcorL) (27), and pea lectin (28), confirming the similarity in three dimensions (Table 2; Fig. 3*B*). Because of the different modes of dimerization, only the monomers were included in the alignment. In the S-lectin the two β-sheets of the monomers extend continuously across the dimer interface. The legume lectins exhibit two other modes of association: (*i*) that of Con A and pea lectin, in which only one β-sheet is continuous and (*ii*) that of EcorL, where a glycosylation site interferes with the formation of the canonical dimer and leads to the formation of a new interface on the opposite edge of the β-sheet, the sheets of the two monomers being roughly perpendicular (27).

The similarity in fold and function suggests an evolutionary relationship between the two lectin families. However, we failed to detect any similarity by the method of Bowie *et al.* (30); this is attributed to insertions of large polypeptide segments in the legume lectins relative to the S-lectin. (*i*) The loop regions of the legume lectins bury one face of the β-sandwich, whereas the equivalent face of the S-lectin is solvated. (*ii*) The additional two N-terminal β-strands of the legume lectins form a different dimer interface. Therefore, the plant lectins and S-lectins use different hydrophobic and hydrophilic residue distributions.

In light of the structural similarity, it is surprising that the location of the carbohydrate-binding sites is topologically

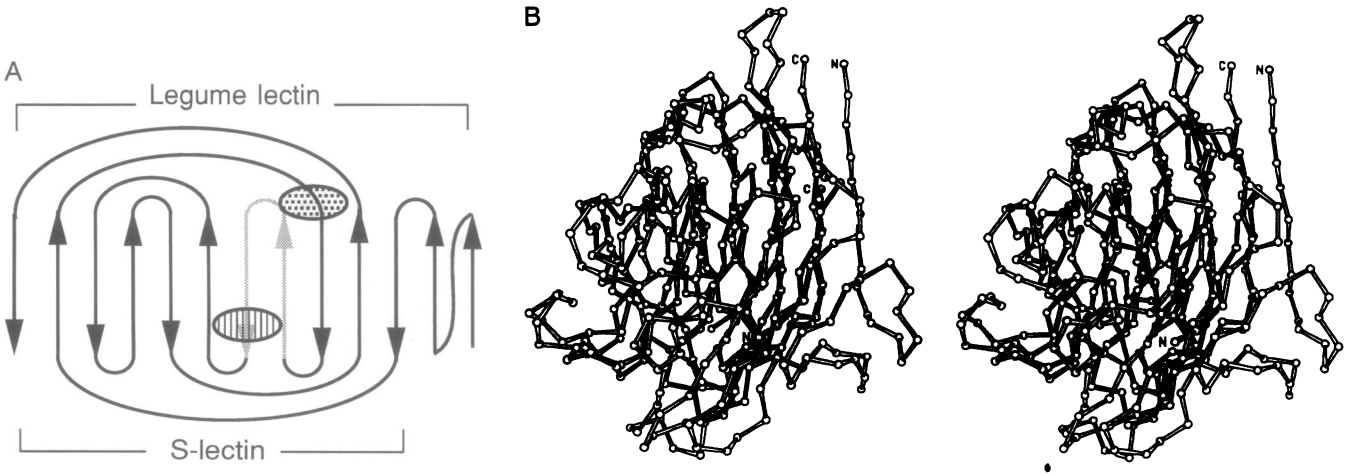

FIG. 3. Comparison between S-lectin and legume lectins. (*A*) Schematic diagram of topology of the two lectin families (the plant-lectin topology corresponds to that of EcorL and pea lectin). The β-hairpin insertion within the jelly roll motif is shown in gray. The ellipsoids show the topological positions of the carbohydrate-binding sites. The ellipsoid filled with vertical lines corresponds to S-lectin, and the ellipsoid filled with dots corresponds to the plant lectins. Note that a residue on the large loop connecting the fifth and sixth strands of the legume lectin also interacts with the sugar (Gly-107 in EcorL); for clarity, this is not shown in the scheme. (*B*) Stereoscopic view of the S-lectin superposed on pea lectin. Virtual bonds between α-carbon atoms of S-lectin are solid, and those between pea lectin are open.

Table 2. Statistics of structure alignment of the 14-kDa S-lectin and three legume lectins

Molecule one	Molecule two	rms* (Å)	rms† (Å)	Identical residues‡
S-lectin	Pea lectin	2.7 (124)	1.9 (103)	10
S-lectin	EcorL	2.8 (125)	1.9 (95)	12
S-lectin	Con A	3.0 (126)	1.9 (84)	6
Pea lectin	EcorL	0.7 (217)		106
EcorL	Con A	1.3 (216)		90
Pea lectin	Con A	1.1 (210)		86
S-lectin(1)	S-lectin(2)	0.5 (132)		132

The program ALIGN, which iteratively accounts for insertion and deletion, was used (29). Only α-carbon atoms were used for the alignment. Brookhaven Protein Data Bank accession number and number of residues in each protein are as follows: S-lectin (1slt), 134; pea lectin (2ltn), 228; EcorL (1lte), 239; Con A (2cna), 237.

*Values are for an alignment that maximizes number of matched amino acid residues; these are listed in parentheses.

†Values are for an alignment that optimizes the match between β-sheets; the number of matched residues is shown in parentheses.

‡Number of identical amino acid residues is based on the structure alignment that maximizes number of matched pairs.

different (Fig. 3*A*) and that the superposed monomers of the S-lectin and legume lectin show the respective sites ≈11 Å apart. The carbohydrate-binding-site architecture is also different, as expected, because divalent cations are required for sugar binding in the legume lectins. All direct protein–carbohydrate interactions involve side chains located on β-strands, unlike the situation in legume lectins, where loop residues are exclusively involved *via* both main-chain and side-chain atoms.

It is intriguing that although in topologically different locations, the carbohydrate-binding sites in both S-lectin and legume lectins involve the β-hairpin insertion (β-strands 4 and 5 of the jelly roll motif). Moreover, in the case of Con A (31) polypeptide shuffling occurs just before this insertion. Whether or not these observations have an evolutionary implication remains to be determined.

Carbohydrate-Binding-Site Interactions. The crystal environments of each of the two S-lectin monomers differ. Nevertheless, the carbohydrate binding is virtually identical, except for a few differences in the solvent structure due to the difference in crystal contacts. The crystal contacts also involve the carbohydrate molecules. The rms in atomic coordinates of the two superposed sugar molecules is 0.3 Å. The values of the ϕ,ψ glycosidic bond torsion angles [defined for the Gal(β1 → 4)GlcNAc linkage by the four atoms as follows: ϕ = O5—C1—O4′—C4′; ψ = C1—O4—C4′—C5′] are −80°, −101° in one monomer and −62°, −102° in the other. The well-defined electron density of both carbohydrate molecules clearly indicates the α-anomeric form for the GlcNAc unit. The 1-OH group is completely solvated such that the β-anomeric form could also be incorporated into the crystal. Thus, the crystal structure does not explain the observed preference. The majority of the interactions are formed between the protein and the galactose component of the disaccharide (Fig. 4). The interactions with the GlcNAc component are less extensive. Most amino acid residues involved in sugar binding are invariant in all sequences of S-lectins. The binding-site depression is shaped to complement the galactose moiety with extensive van der Waals contacts and a network of electrostatic interactions (Fig. 4). In addition, a water molecule mediates the interactions of the side chain of Asn-46 with the 3-OH and 4-OH of galactose. The aromatic side chain of the conserved Trp-68 stacks adjacent to the galactose ring. Such van der Waals interactions between sugar and aromatic side chains are quite common in protein–carbohydrate complexes (32). The interaction of the hydrophobic part of the side chain of the conserved Lys-63 with the other face of the aromatic ring of Trp-68 assures its optimal orientation (Fig. 1).

The axial 4-OH of galactose, a main determinant of the S-lectin specificity, forms two key electrostatic interactions; one with the N^{η} atom of Arg-48 and the other with the N^{ε} atom of His-44. Both are invariant residues in the sequences of S-lectins (Fig. 4). The mean distances to the nitrogen atoms (averages for the two monomers) are 2.9 Å and 2.8 Å, respectively. The $O^{\delta 1}$ of Asn-46 and a water molecule also form electrostatic interactions with 4-OH, with mean distances of 3.2 Å and 3.1 Å, respectively. The interaction with Arg-48 and geometrical considerations suggest that the 4-OH is oriented away from Arg-48, most probably toward His-44. This orientation is possible only if the N^{ε} atom of His-44 is not protonated upon binding. Modeling shows that the disposition of the Trp-68 side chain is consistent only with an axial 4-OH because an equatorial group would introduce unacceptable short contacts. It would, in addition, be impossible to form the electrostatic interactions. Modifications are also excluded at position 6 due to the close contact of C6 with Trp-68 and to the interaction of the 6-OH group with the side chain of Asn-61. Modifications at C3 have fewer restrictions. The 3-OH group has only one water-mediated hydrogen-bonding interaction with the protein. The C2 position is also unrestricted, with the 2-OH completely solvated. These results agree with binding studies permitting chemical modifications at positions 2 and 3 but not at positions 4 and 6 (14).

Glu-71 and Arg-48 interact with both pyranose rings, thus determining their precise orientation. The interactions of the GlcNAc moiety with the protein are less extensive than those

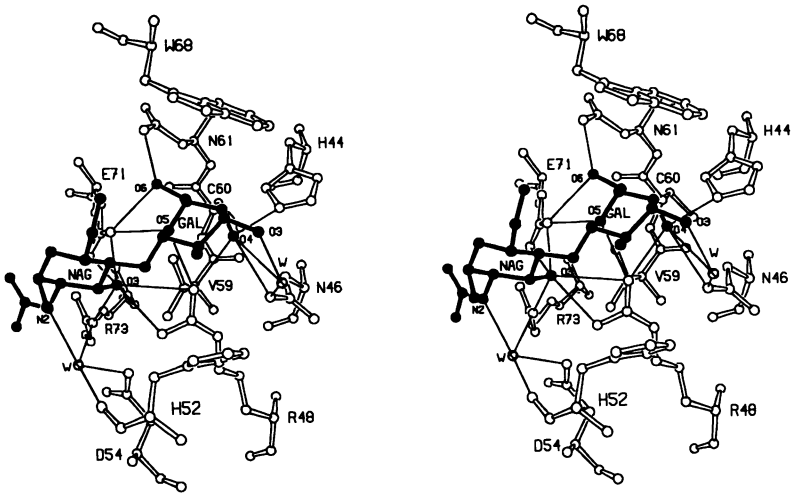

FIG. 4. Stereoscopic representation of the S-lectin carbohydrate-binding site. Bonds between carbohydrate atoms are solid, and those between protein atoms are open. The electrostatic interactions between protein and sugar atoms are shown in thin lines. For clarity, protein–protein electrostatic interactions of residues involved in sugar binding are not indicated; these include the salt bridges between Arg-48 and Asp-54, Arg-73 and Asp-54, and Arg-73 and Glu-71. Also not indicated are electrostatic interactions that help orienting protein groups optimally to interact with sugar atoms: Asn-33 $O^{\delta 1}$ with His-44 $N^{\delta 1}$, Arg-111 N^{η} with Asn-61 $O^{\delta 1}$, Arg-48 N^{ε} with Asn-46 $O^{\delta 1}$, Asn-46 $N^{\delta 2}$ with Phe-30 O, and Asn-46 $N^{\delta 2}$ with Ser-29 O^{γ}.

of galactose. They are mainly mediated through the contact of the 3-OH group with Arg-73, Arg-48, and Glu-71. In addition, the N2 atom of the N-acetyl group is involved in a water-mediated interaction with the side chains of Arg-73 and Asp-54 and with the main-chain carbonyl of His-52. The binding of *N*-acetyllactosamine to S-lectin is ≈5-fold tighter than the binding of lactose (33, 34). This result may be attributed to van der Waals interactions between the N-acetyl group and the side chains of Arg-73 and Glu-71.

The carbohydrate–protein interactions are supported by exquisite protein–protein electrostatic interactions, assuring optimal side-chain conformations (Fig. 4). Most striking is the spatial disposition of the charged residues Arg-48, Asp-54, Arg-73, and Glu-71, which together form a network of three salt bridges unprecedented in other sugar-binding proteins of known structure. Other important hydrogen bonds are listed in the legend to Fig. 4. Of these, Asn-46, Glu-71, and Arg-73 have been previously suggested as essential for binding by site-directed mutagenesis (14). These structural data explain why those amino acid residues that are directly and indirectly associated with the carbohydrate binding are conserved.

Environment of Thiol Groups. The crucial role that the oxidation states of the S-lectin thiol groups play in regulating function *in vivo* is unclear (11). In the refined structure at 1.9-Å resolution, the thiol groups of Cys-42 and Cys-60 are reduced and buried. The thiol group of Cys-2 is disordered, and those of Cys-16, Cys-88, and Cys-130 are oxidized and solvated. Structural considerations suggest that none of the six cysteine residues is required for binding activity. No thiol group is directly involved in sugar binding, and all thiol groups bind heavy atoms without impairing sugar binding. Cys-60 is the only cysteine close to the binding site. Its main-chain atoms are involved in the formation of the active-site depression, and its side chain is buried and surrounded by hydrophobic residues. Nevertheless, this cysteine was also observed to be accessible to heavy-atom reagents. Site-directed mutagenesis studies of the 14-kDa S-lectins, replacing Cys-60 and Cys-2 by serine residues, did not inhibit sugar binding, consistent with the structural information (13, 14).

The crystal contacts may protect the structure integrity. Therefore, it should not be concluded that the cysteine oxidation observed in this crystal structure would not effect sugar binding in solution. Whether thiol group oxidation directly damages the carbohydrate-binding site or whether inactivation is the result of long-range effects, such as perturbation of the overall fold or formation of disulfide bonds that hinder access to the binding site, cannot be currently ascertained. These questions may be better addressed after the structure determination of the sugar-free form in the reduced and oxidized states.

We thank Drs. John Moult, Gary Gilliland, and Christian Sander for useful discussions. Crystallographic work by D.-I.L., G.K., and O.H. was supported by National Science Foundation Grant DMB-9019340 and National Institutes of Health Grant RO1-AI27175 to O.H. Work by H.A. and G.R.V. was supported by National Science Foundation Grant MCB-9105875 to G.R.V.

1. Drickamer, K. (1988) *J. Biol. Chem.* **263,** 9557–9560.
2. Harrison, F. L. (1991) *J. Cell Sci.* **100,** 9–14.
3. Cooper, N. W. & Barondes, S. H. (1991) *J. Cell Biol.* **110,** 1681–1691.
4. Feizi, T. & Childs, R. A. (1987) *Biochem. J.* **245,** 1–11.
5. Do, K. Y., Smith, D. F. & Cummings, R. D. (1990) *Biochem. Biophys. Res. Commun.* **173,** 1123–1128.
6. Zhou, Q. & Cummings, R. D. (1990) *Arch. Biochem. Biophys.* **281,** 27–35.
7. Hughes, R. C. (1992) *Biochem. Soc. Trans.* **20,** 279–284.
8. Cooper, D. N. W., Massa, S. M. & Barondes, S. H. (1991) *J. Cell Biol.* **115,** 1437–1448.
9. Sato, S. & Hughes, R. C. (1992) *J. Biol. Chem.* **267,** 6983–6990.
10. Wells, V. & Mallucci, L. (1991) *Cell* **64,** 91–97.
11. Kasai, K. (1990) in *Advances in Lectin Research*, ed. Franz, H. (Volk Gesundheit, Berlin), Vol. 3, pp. 10–35.
12. Clerch, L. B., Whitney, P. L., Hass, M., Werner, R. & Massaro, D. (1988) *Biochemistry* **27,** 692–699.
13. Abbott, W. M. & Feizi, T. (1991) *J. Biol. Chem.* **266,** 5552–5557.
14. Hirabayashi, J. & Kasai, K. (1991) *J. Biol. Chem.* **266,** 23648–23653.
15. Howard, A. J., Gilliland, G. L., Finzel, B. C., Poulos, T., Ohlendorf, D. O. & Salemme, F. R. (1987) *J. Appl. Crystallogr.* **20,** 383–387.
16. Steigemann, W. (1974) Doctoral thesis (Technical University, Munich).
17. Jones, T. A. (1982) in *Computational Crystallography*, ed. Sayre, D. (Oxford Univ. Press, London), pp. 303–317.
18. Jones, T. A. & Thirup, S. (1986) *EMBO J.* **5,** 819–822.
19. Brünger, A. T., Kuriyan, J. & Karplus, M. (1987) *Science* **235,** 458–460.
20. Tronrud, D. E., TenEyck, L. F. & Matthews, B. W. (1987) *Acta Crystallogr.* **A43,** 489–501.
21. Abbott, W. M., Mellor, A., Edwards, Y. & Feizi, T. (1989) *Biochem. J.* **259,** 283–290.
22. Kabsch, W. & Sander, C. (1983) *Biopolymers* **22,** 2577–2637.
23. Weis, W. I., Kahn, R., Fourme, R., Drickamer, K. & Hendrickson, W. A. (1991) *Science* **254,** 1608–1615.
24. Becker, J. W., Reeke, G. N., Jr., Wang, J. I., Cunningham, B. A. & Edelman, G. M. (1975) *J. Biol. Chem.* **250,** 1513–1524.
25. Reeke, G. N., Jr., Becker, J. W. & Edelman, G. M. (1975) *J. Biol. Chem.* **250,** 1525–1547.
26. Hardman, K. D., Agrawal, R. C. & Freiser, M. J. (1982) *J. Mol. Biol.* **157,** 69–86.
27. Shaanan, B., Lis, H. & Sharon, N. (1991) *Science* **254,** 862–866.
28. Einspahr, H. M., Parks, E. H., Suguna, K., Subramanian, E. & Suddath, F. L. (1986) *J. Biol. Chem.* **261,** 16518–16527.
29. Satow, Y., Cohen, G. H., Padlan, E. A. & Davies, D. R. (1986) *J. Mol. Biol.* **190,** 593–604.
30. Bowie, J. U., Lüthy, R. & Eisenberg, D. (1991) *Science* **253,** 164–170.
31. Carrington, D. M., Auffret, A. & Hanke, D. E. (1985) *Nature (London)* **313,** 64–67.
32. Vyas, N. K. (1991) *Curr. Opin. Struct. Biol.* **1,** 732–740.
33. Leffler, H. & Barondes, S. (1986) *J. Biol. Chem.* **261,** 10119–10126.
34. Ahmed, H., Allen, H. J., Sharma, A. & Matta, K. L. (1990) *Biochemistry* **29,** 5315–5319.